

# VEET Ambient Light Sensor Lux Characterization

# Table of Contents

Table of Contents	2
Introduction	2
Glossary of Terms and Abbreviations	3
Fundamentals of Lux and Spectral Mismatch	4
Spectral Irradiance and Spectral Power Distribution	4
Device Spectral Response vs. Photopic Ideal	4
Example: LED Color and Prediction Error	5
Data Collection	8
Light Sources and Environments	8
Measurement Setups	8
Trusted Devices	8
Integration Time and Gain Normalization	13
The Lux Characterization Equation	13
Spectrilight Predicted VEET Counts	13
Scaling Predicted Counts to Match VEET ALS Output	15
Device Glass Factor and Counts per lux	18
Estimating Device Glass Factor	18
Custom Lux Equation	20
Firmware Formulation	23
Model Error Analysis	24
Agreement with Trusted Lux (Log-Log Domain)	24
Spectral Dependency of Lux Predictions	25
Challenges with Mixed or Atypical Lighting	27
Device-to-Device Variation (Not Included)	27
Physical Measurement Differences	27
Conclusion	28

## Introduction

The Visual Environment Evaluation Tool (VEET) is a pair of temple arms equipped with four sensors that enable researchers to gather data on characteristics of light near the eye. This document provides insight into the characterization equation that converts counts from one of its sensors—the Ambient Light Sensor (ALS)—into photometric lux units.

While each VEET undergoes unit-specific calibration to translate raw counts into standardized internal units, an additional step is required to convert these values into lux—a photometric quantity weighted by the sensitivity of the human eye.

Although the ALS sensor includes a photopic filter, its spectral response does not perfectly match that of the human eye. As a result, the lux conversion cannot rely on a single scale factor.

Furthermore, the device's optical stack—the diffuser, housing, and protective window—can shift or attenuate portions of the spectrum, introducing additional variability.

To account for these effects, the firmware applies a characterization equation that corrects for spectral differences as a function of light type and color temperature. The following sections introduce the fundamentals of the lux calculation, highlight the causes of spectral mismatch, and describe the data collection and modeling methods used to derive and validate the equation.

## Glossary of Terms and Abbreviations

ALS	Ambient Light Sensor. Measures visible and infrared light to estimate environmental brightness.
Basic Counts	Sensor counts normalized for gain and integration time.
$C_0, C_1$	Empirical coefficients used in the lux equation to weight infrared (IR) and visible (VIS) channels contributions.
CCT	Correlated Color Temperature: a descriptor of how warm (yellow/red) or cool (blue) a light source appears.
CIE	Commission Internationale de l'Éclairage: International Commission on Illumination
CPL	Counts (basic) per lux
DGF	Device Glass Factor: Scalar to correct for optical attenuation.
Golden Unit	The VEET device that has unit to unit calibration ratios of 1.0.
lux	A photometric unit representing luminous flux per unit area, weighted by the sensitivity of the human eye.
IR Channel	Infrared photodiode channel—used in spectral correction.
IR/VIS Ratio	The ratio of infrared (IR) to visible (VIS) counts—used as a proxy for spectral shape or color temperature.
SPD	Spectral Power Distribution.
VIS Channel	Visible light photodiode channel—filtered to approximate the CIE photopic response.

## Fundamentals of Lux and Spectral Mismatch

The following section explains how lux is physically defined and why a mismatch between ideal photopic response and sensor response can cause systematic error.

### Spectral Irradiance and Spectral Power Distribution

Light from a source can be described by its Spectral Power Distribution (SPD),  $E(\lambda)$ , which gives the irradiance ( $\text{W/m}^2/\text{nm}$ ) as a function of wavelength. Lux, however, is computed by weighting the spectral energy according to the photopic response of the human eye,  $V(\lambda)$ , scaled by a luminous efficacy constant:

$$\text{lux} = 683 \int_{380}^{780} E(\lambda) \cdot V(\lambda) d\lambda$$

This integral emphasizes green-yellow wavelengths around 555 nm and deemphasizes energy in the blue and red.

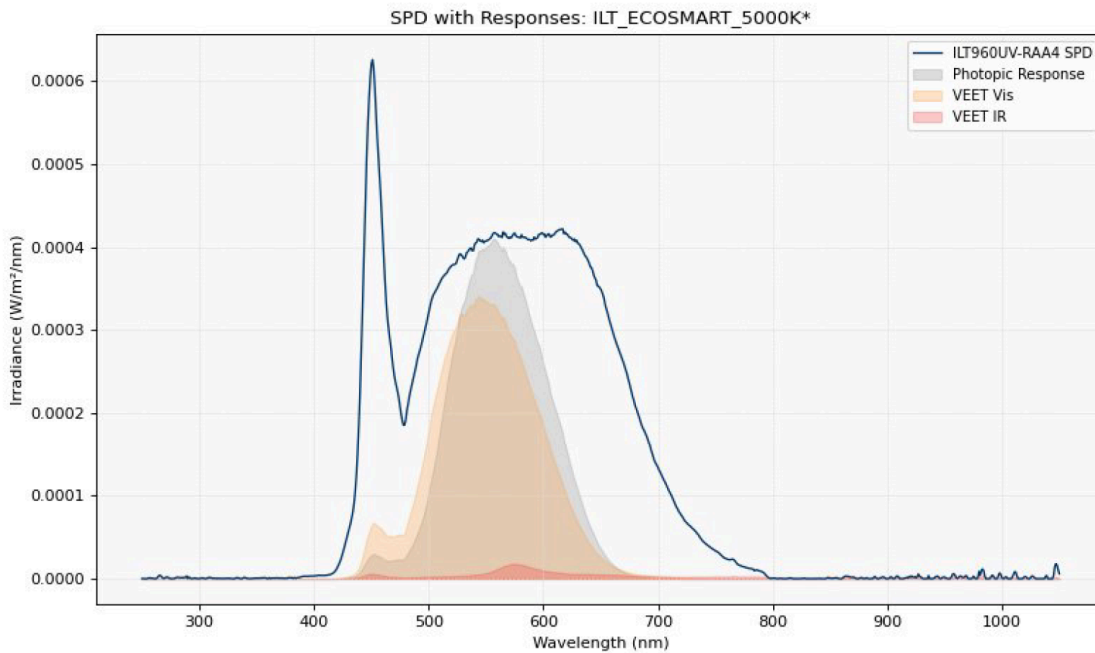


**Figure 1:** Example SPD with weighted photopic curve; the shaded area represents the lux integral.

### Device Spectral Response vs. Photopic Ideal

The ALS sensor's VIS channel has a photopic mask that is designed to approximate the spectral response of the human eye,  $V(\lambda)$ . However, this match is not perfect, and additional deviations are introduced by VEET's optical stack—the diffuser, protective window, and housing. Deviations from ideal response are due to effects such as the following:

- **Infrared tail:** Leakage of near-infrared light through the VIS mask, resulting in signal contributions outside the photopic range.
- **Spectral shift:** Misalignment of the VIS peak sensitivity compared to the ideal photopic curve, caused by both sensor design and optical stack-induced distortion.
- **Peak attenuation:** Reduction in signal strength at the peak photopic wavelengths due to absorption or scattering within the optical stack.

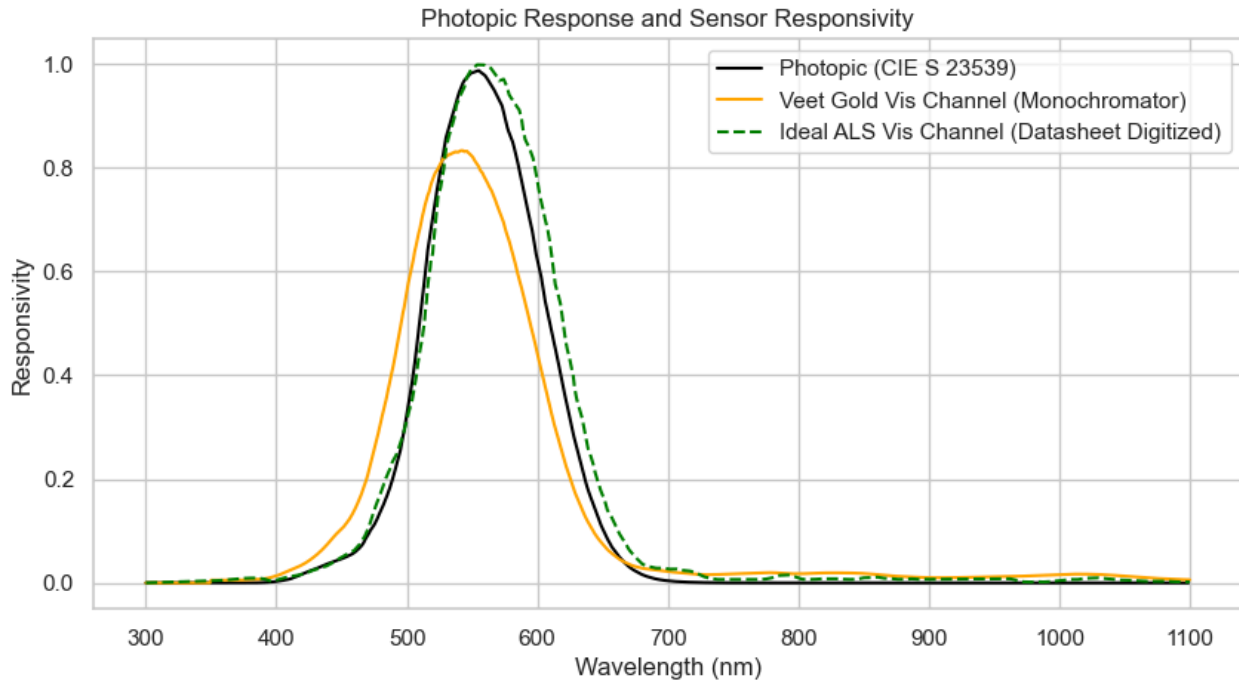


**Figure 2:** Comparing ideal photopic response, ideal sensor response, and VEET's measured response.

## Example: LED Color and Prediction Error

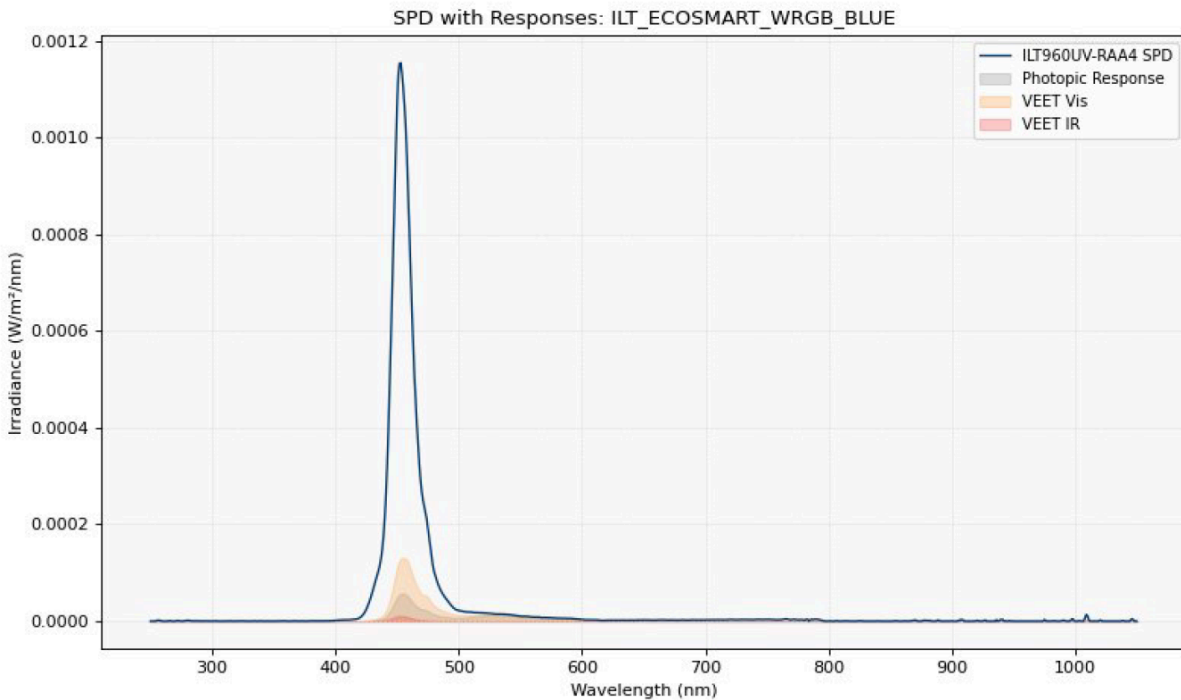
To illustrate how spectral mismatch contributes to lux prediction error, Figure 3 compares the device-weighted response and the ideal photopic response under three different LED spectral power distributions (SPDs): blue, green, and red. In each plot, the shaded orange region represents the weighted VEET response—the area under the device's responsivity curve multiplied by the SPD—while the shaded gray region represents the photopic-weighted response used in the lux calculation. By comparing the relative areas under these curves, we observe how prediction error arises due to differences in spectral alignment:

- **Blue LED:** Shows significant **overprediction**, with much of the device response falling outside the photopic response.
- **Red LED:** Shows significant **underprediction**, with the device response contributing less than what is captured by the photopic response.
- **Green LED:** Shows relatively **minimal error**, as its SPD aligns more closely with both the device and photopic response peaks.

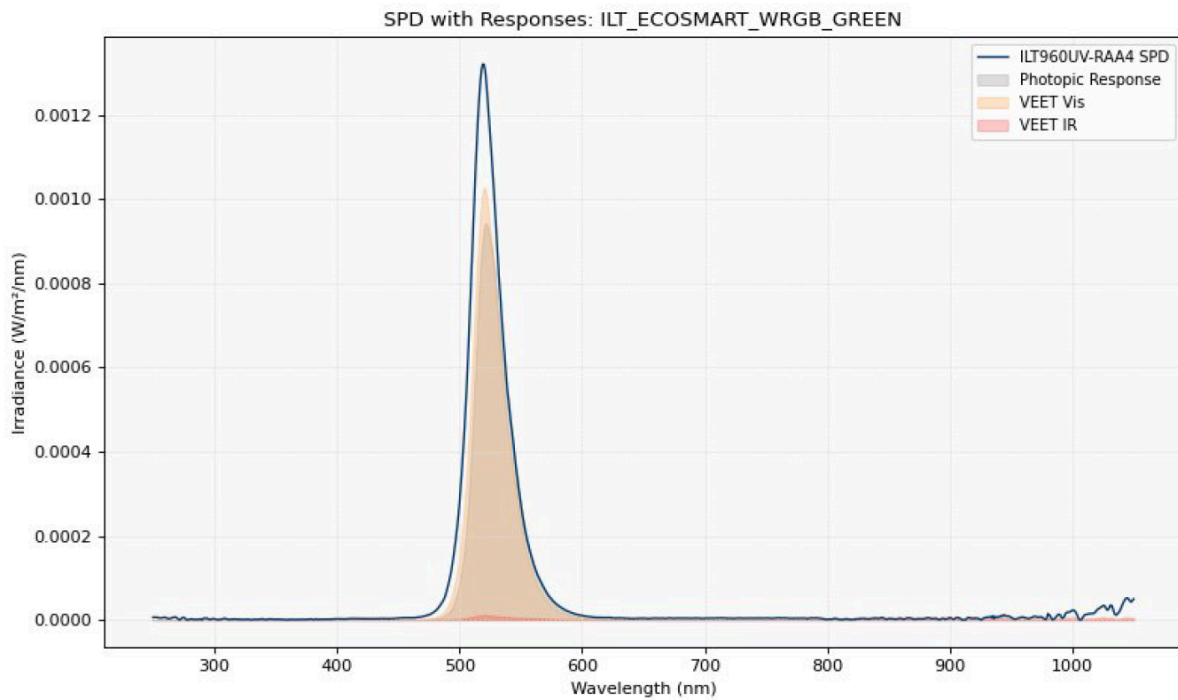
It's important to emphasize that accurately predicting lux from single-color LEDs is not the goal of this model. Rather, these examples serve to illustrate how the shape and spectral position of the SPD—driven by the light source's type, color or correlated color temperature (CCT)—can strongly influence both the magnitude and direction of prediction error.

This sensitivity to spectral variation is the core reason for developing a characterization equation: to correct for these errors across a wide range of real-world lighting conditions, where SPDs vary continuously across the visible and near-infrared spectrum.

## BLUE LED



## GREEN LED



## RED LED

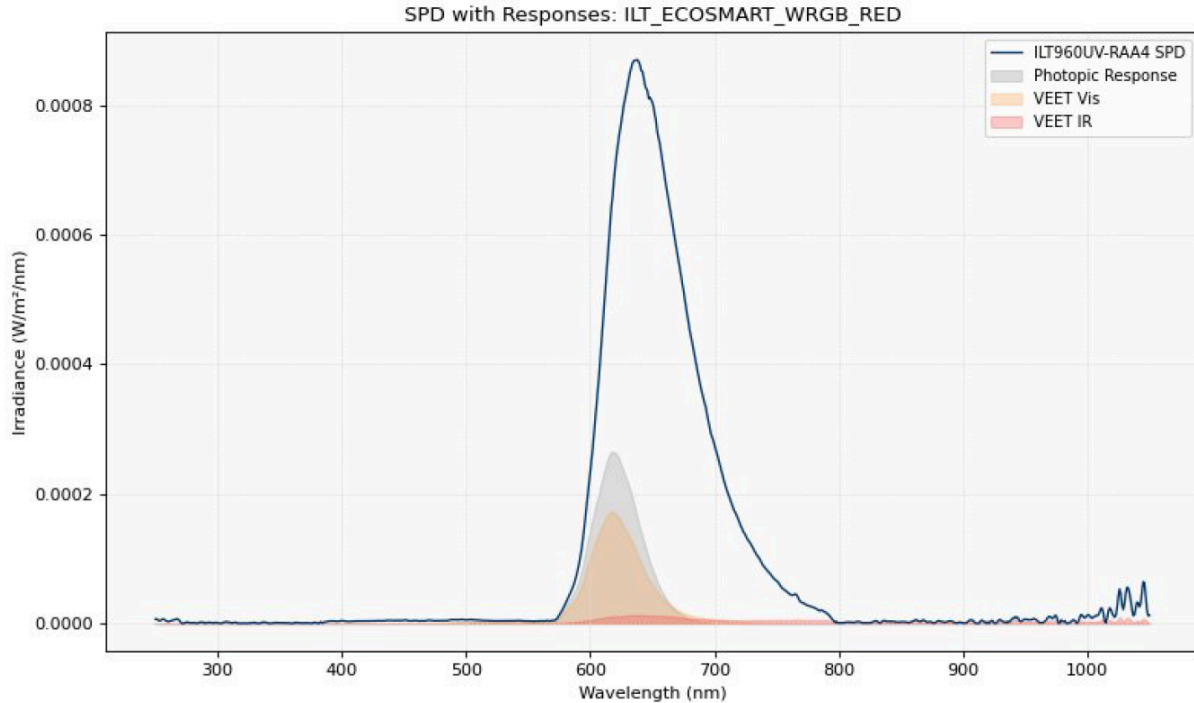


**Figure 3:** Comparison of ALS VEET-weighted response (shaded orange area) and photopic-weighted response (shaded gray area) under blue, green, and red LED spectral power distributions (SPDs).

## Data Collection

To build and validate the lux characterization model, data was collected for all common light sources.

## Light Sources and Environments

Data was collected from the following sources:

- LED and RGB
- Fluorescent
- Incandescent and halogen
- Daylight (outdoor scenes)
- Daylight through glass

## Measurement Setups

Multiple setups were used to isolate effects of spectral variation and optical geometry:

- **Polychromator dark room:** The polychromator was used to recreate target spectra, which were projected into an integrating sphere. This is the most precise method, though it is limited to the 380 -780 nm range. Target spectra were sourced from the following:
  - Built-in UT-Spectra polychromator library
  - Python Colour-Science library spectral datasets
  - Measured light sources using the Spectrilight ILT960
- **Darkbox setup:** A dark box with an aperture and diffuser allowed targeted exposure to bright IR-rich sources such as halogen and incandescent lights. This setup provided the most reliable IR content.
- **Tripod mounted open air setup:** Devices were mounted on the same fixture, on a tripod, for ambient scene measurement.
- **Tripod mounted open air setup with Field of View (FOV) restriction:** Aperture tubes were added to each sensor to restrict their field of view to a 30° full cone, reducing scene variability.
- **Cone diffuser lightbox:** Based on the open-air FOV-restricted setup, this configuration placed apertures inside a lightbox aimed at overlapping regions of a diffuser sheet, improving light field uniformity.

When comparisons or correlations across multiple devices were required, only Polychromator, and Dark Box data were used to ensure consistency. Open-air, FOV-restricted, and lightbox were only used for single device observations.

## Trusted Devices

To obtain trusted lux measurements and SPD measurements, the following instruments were used:

- **Konica Minolta CL500a:** A spectrophotometer that reports lux, CCT, and visible-range SPD. Initially preferred for lux reference, but its wide FOV often conflicted with the VEET's narrower FOV, especially in directional or mixed-light conditions.

- **ILT Spectrilight ILT960:** A spectroradiometer covering 300–1050 nm used to capture SPDs and compute lux via photopic integration. It provided a consistent reference across both visible and near-infrared ranges.

The CL500a was the first choice for trusted lux measurement; however, FOV differences between the CL500a and the ALS often led to inconsistent results, especially under directional or mixed lighting. Attempts to match FOV using apertures and diffuser cones improved consistency of the agreement but introduced a new source of variability.

To address this, the final modeling approach captured SPDs with the Spectrilight, which was then used to calculate both trusted lux (via photopic integration) and predicted ALS counts (via sensor response simulation), enabling the use of a single device for a light source and ensuring matched optical paths and consistent modeling inputs.

Although the CL500a was initially the preferred reference for lux, consistent agreement proved difficult due to FOV mismatches. Efforts to constrain the FOV using apertures and diffuser cones improved alignment but introduced new sources of variability.

As a result, the final modeling approach relied on SPDs captured with the Spectrilight ILT960 to compute both of the following:

- Trusted lux, via integration with the photopic response curve.
- Predicted ALS counts, via application of the golden unit's spectral responsivity curve.

This method, outlined in Section 7, enabled consistent modeling by using a single optical path, removing geometric variability between devices and improving the reliability of lux estimation under controlled conditions.

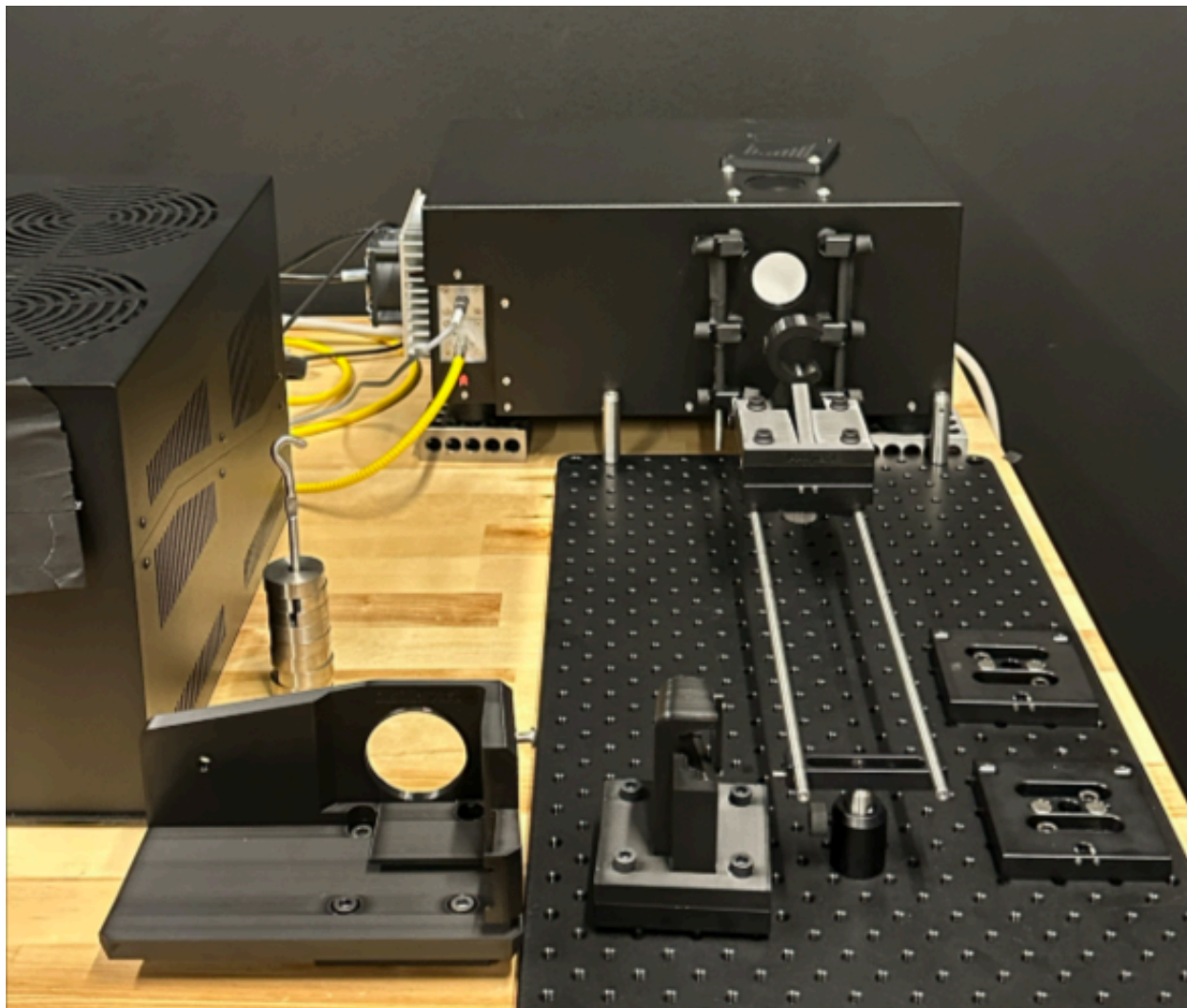


**Figure 4:** *Controlled spectral characterization setup using a polychromator and integrating sphere.*

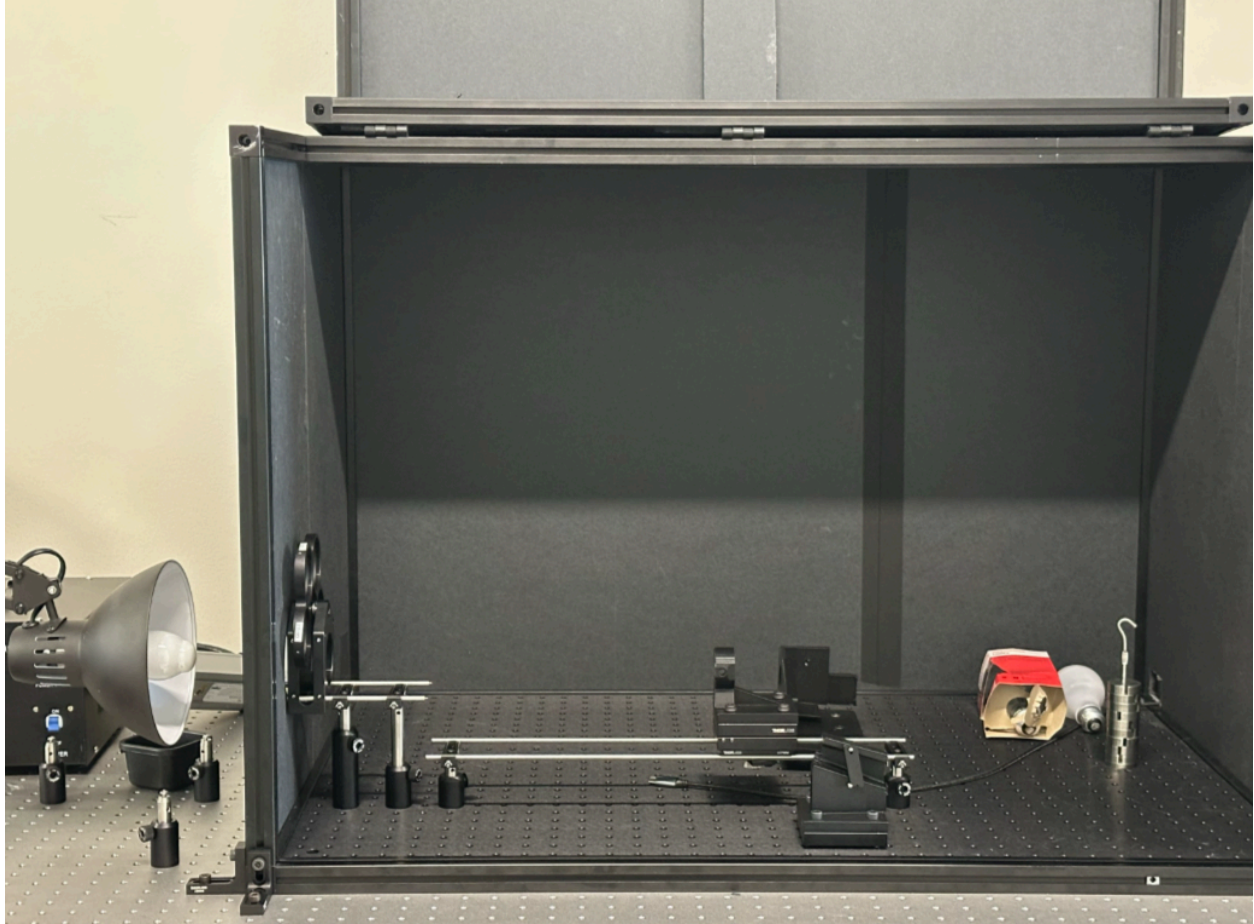


**Figure 5:** Enclosed setup with a diffuser and aperture used to isolate halogen and incandescent sources.



**Figure 6:** A hybrid test configuration combining controlled field-of-view restriction with uniform diffuse illumination.

## Integration Time and Gain Normalization

Raw counts from the ALS sensor are influenced by both integration time and gain settings. To enable consistent interpretation across devices and lighting conditions, the sensor firmware normalizes the VIS and IR channel readings prior to applying the lux characterization equation.

The normalization process involves the following:

- **Gain correction:** Each channel's raw counts are divided by its corresponding gain ratio. Gain settings are hardware-defined and indexed in firmware for onboard lux calculation.
- **Integration time normalization:** Corrected counts are scaled by integration time (in seconds), yielding a time-normalized count.

Counts that have been both normalized for gain and integration time are referred to as **basic counts**.

## The Lux Characterization Equation

The goal of the characterization model is to convert normalized ALS signals into an estimate of photometric lux. The lux equation recommended by the sensor manufacturer takes the following form:

$$lux = \frac{C_0 VIS_{norm} \cdot C_1 IR_{norm}}{DGF \cdot A_{time}}$$

- $VIS_{norm}, IR_{norm}$ : Gain normalized sensor counts from the visible and infrared channels
- $A_{time}$ : Integration time in milliseconds
- $DGF$ : Device Glass Factor (unit-specific scalar to account for optical stack and enclosure attenuation)
- $C_0, C_1$ : Empirical coefficients tuned to correct for spectral mismatch, varying with IR/VIS ratio.

Because the sensor's spectral response does not perfectly match the photopic curve, the coefficients  $C_0$  and  $C_1$  cannot be treated as fixed values. Instead, they are determined through a piecewise curve fit across different IR/VIS ratio domains, where the IR/VIS ratio serves as a proxy for color temperature and overall spectral shape. This allows the model to adapt its weight dynamically based on the type of light source and, by extension, the spectral shape.

## Spectrilight Predicted VEET Counts

To enable accurate model training and lux prediction, the ALS sensor response is simulated under a known SPD. The VIS and IR counts under each lighting condition are predicted using SPD measurements from the Spectrilight ILT960 and a measured VEET responsivity curve.

These values represent the expected VEET response to the measured spectrum—free from FOV mismatch or ambient scene variability.

The device responsivity curve used for these simulations was obtained from the golden VEET unit, which serves as the reference device for all characterization work. This golden unit was used consistently for the following:

- Predicted counts scaling
- Device Glass Factor (DGF) coefficient fitting
- All model validation

The spectral responsivity was measured using a monochromator sweep, exposing the golden unit to narrowband light across the visible and near-infrared spectrum. This generated response curves for both the VIS and IR channels, capturing the full effect of the sensor's optical stack.

Importantly, the golden unit is also the reference device for device-to-device calibration; it is assigned a calibration scaling factor of 1.0 for all channels. All other units in the system are calibrated relative to this device, meaning its predicted responses define the baseline against which other devices are scaled.

This simulation strategy provides several key advantages:

- It minimizes inconsistencies caused by FOV mismatch between the VEET and external references.
- It ensures a shared optical path between lux integration and ALS count prediction, while still accounting for effects from VEET optical stack.
- Adding additional light sources to the characterization dataset only requires the SPD.

The resulting predicted ALS counts serve as the basis for estimating DGF and the piecewise lux characterization model.

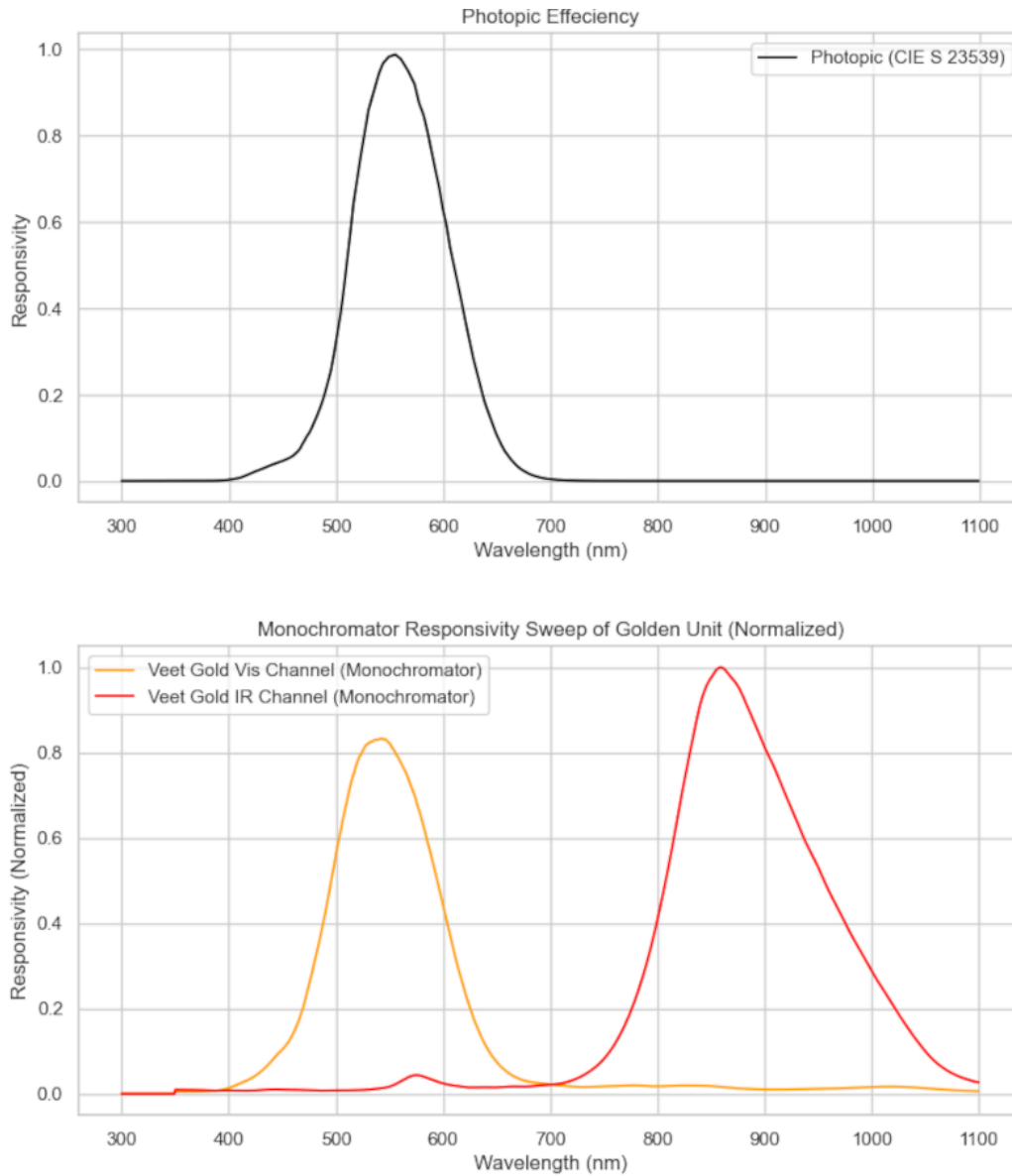


**Figure 7:** Response curves used for lux calculation and device response prediction. Top: The CIE photopic luminosity function  $V(\lambda)$ , used to compute lux from SPD measurements. Bottom: The VIS and IR channel responsivity curves from the golden unit, measured via monochromator sweep.

## Scaling Predicted Counts to Match VEET ALS Output

To use the predicted VIS and IR counts from the Spectrlight SPD data in model development, it is necessary to scale them to match the actual counts measured from the ALS device.

To make the predicted counts compatible with real device measurements and integration times, we define a basic counts form by dividing ALS counts by integration time. Predicted counts are then scaled using empirical constants:

$$\frac{IR_{norm}}{A_{time}} = \alpha \cdot IR_{pred} \Rightarrow IR_{pred,basic} = \alpha \cdot IR_{pred} \cdot A_{time}$$

$$\frac{VIS_{norm}}{A_{time}} = \beta \cdot Vis_{pred} \Rightarrow VIS_{pred,basic} = \beta \cdot Vis_{pred} \cdot A_{time}$$

- $IR_{norm}, VIS_{norm}$  : gain corrected ALS counts
- $IR_{basic}, VIS_{basic}$  : gain and time corrected ALS counts (basic counts)
- $IR_{pred}, VIS_{pred}$  : predicted counts based on SPD and response curves
- $A_{time}$  : integration time in milliseconds.
- $\alpha, \beta$  : empirical scaling factors derived by matching predicted and measured counts across a range of lighting conditions

To ensure accurate alignment between predicted and measured counts, the scaling factors  $\alpha$  and  $\beta$  were derived from separate, channel-specific datasets. This approach was chosen to best match each channel's spectral sensitivity and to minimize geometric variability:

- For VIS scaling ( $\alpha$ ), only polychromator measurements were used. This source provides stable, uniform illumination concentrated in the visible band, making it well-suited for accurately characterizing the response of the VIS channel.
- For IR scaling ( $\beta$ ), only high-IR light sources measured in the dark box were used. These sources provided strong infrared content and were measured under stable, uniform lighting with a constrained field of view.

By selecting data with well-aligned spectral content and consistent light geometry, this fitting strategy ensured that the scaling factors accurately reflect the underlying sensor response under idealized conditions. The regression fits used to determine the scaling factors  $\alpha$  (for VIS) and  $\beta$  (for IR) are shown in Figure 8, where the slopes of the respective trendlines correspond to the final scaling coefficients applied throughout the model.

## Spectrilight Prediction vs ALS Observation Across Channels

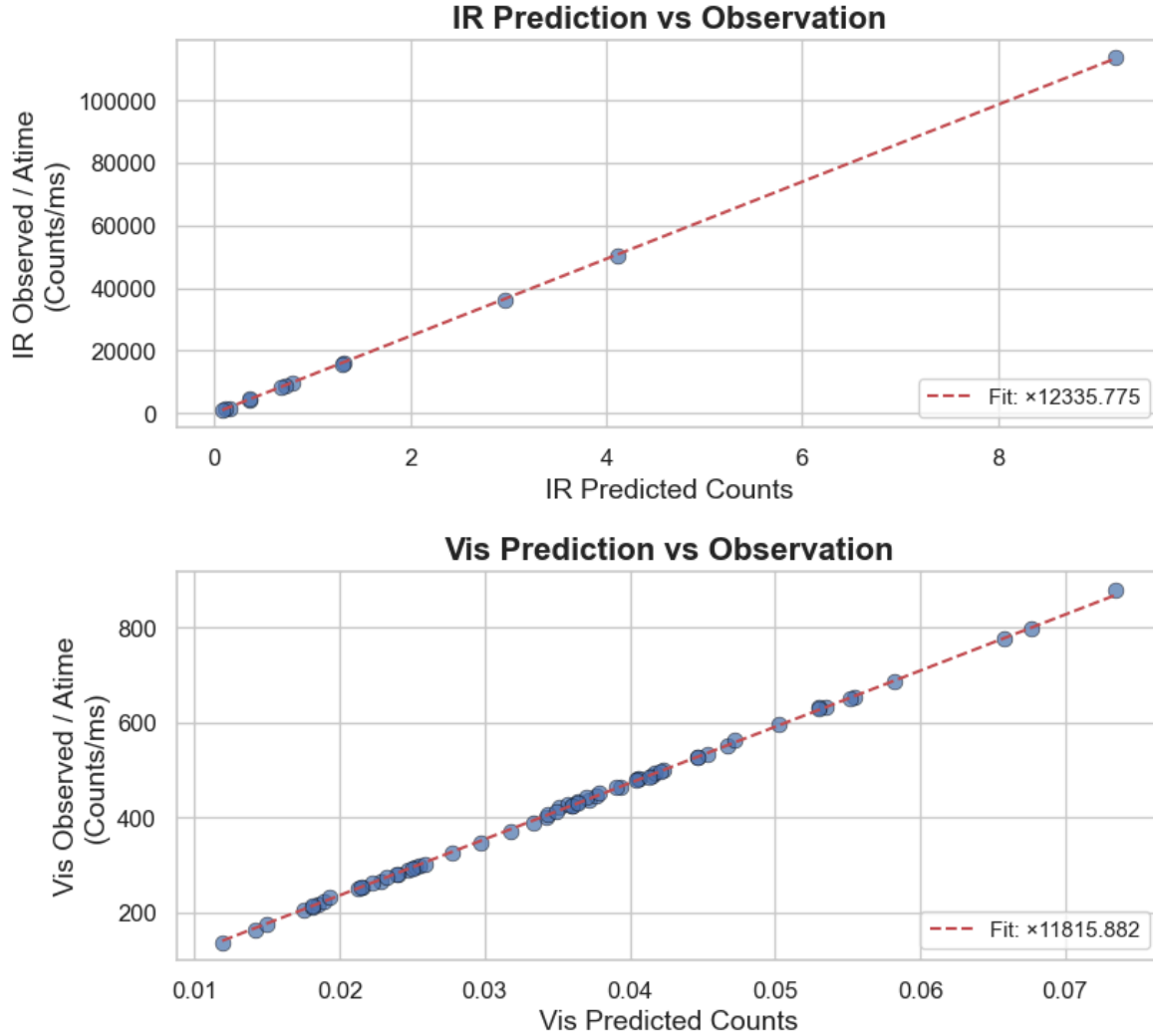


**Figure 8:** Regression fits for deriving predicted-VEET scaling coefficients. Top: IR scaling ( $\beta$ ) based on high-IR darkbox sources. Bottom: VIS scaling ( $\alpha$ ) based on polychromator data. Each plot shows predicted VEET counts from Spectrilight (x-axis) versus ALS basic counts (y-axis), with the slope of the fit line representing the scaling coefficient.

## Device Glass Factor and Counts per lux

The Device Glass Factor (DGF) is a scaling term in the lux characterization equation that accounts for signal loss due to the optical stack, including the diffuser, protective window, and any aperture restrictions. It represents how much the device's physical design attenuates incoming light relative to the ideal sensor response.

$$DGF = \frac{\text{lux} \cdot A_{\text{time}}}{VIS_{\text{norm}}} \left[ \frac{\text{lux} \cdot \text{ms}}{\text{counts}} \right]$$

Counts per lux (CPL), as defined by manufacturer application notes, is the normalized counts per lux at a particular integration time and is related to DGF by integration time.

$$CPL = DGF \cdot A_{\text{time}} \left[ \frac{\text{counts}}{\text{lux}} \right]$$

While it is mathematically possible to absorb DGF into the spectral correction coefficients  $C_0$  and  $C_1$ , doing so distorts their physical meaning by mixing spectral weighting with optical scaling. Separating these terms allows the coefficients to remain tied to spectral correction, while DGF and CPL remain tied to optical and integration-time-dependent scaling. This separation also makes CPL meaningful and easier to use when adjusting the model for varying integration times.

### Estimating Device Glass Factor

To estimate DGF, the optical scaling effect is isolated by using a light source with a flat spectrum. Illuminant E was selected for this purpose due to its equal-energy distribution, which minimizes errors from spectral mismatch. DGF is computed by dividing the predicted VIS basic counts by the trusted lux value for this source:

$$DGF = \frac{VIS_{\text{pred,basic,IllumE}}}{\text{lux}_{\text{IllumE}}} = \frac{243.60}{14.62} = 16.67$$

This DGF value is then used across all subsequent modeling and is the basis for calculating CPL at any integration time.

## Light Source Datasheet: UT\_Illuminant\_E

UUID: 3cc6ab15-0c1f-49c8-b5dc-3031c9f153c7

Source Type: STD ILLUM - equal energy

Measurement Time Stamp: 2025-04-23 16:00:00

CCT (Spectrilight): 5544.84448433 K

Lux (Veet ALS est): 17.21

Lux (Spectrilight): 14.62

Lux (CL500A): 14.59

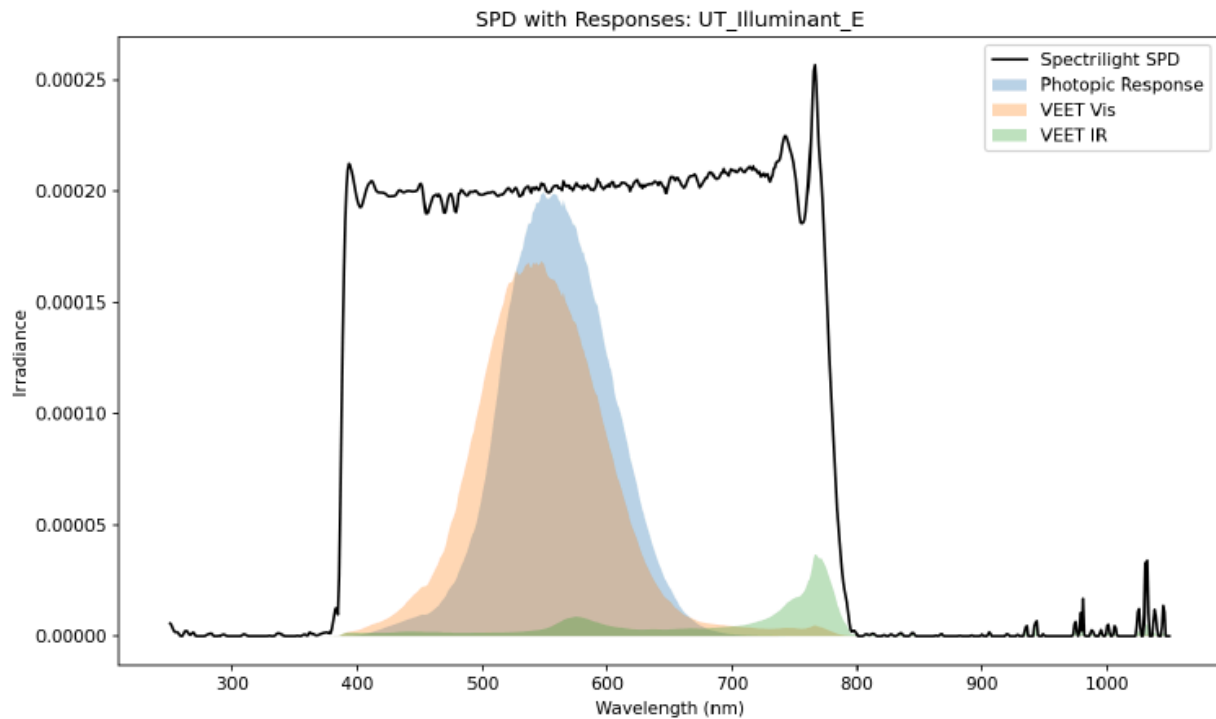


**Figure 9:** Light source summary for Illuminant E. This summary includes the measured SPD, predicted sensor responses from the golden unit, calculated photopic area used for lux, and relevant metadata. Illuminant E is used as the reference condition for estimating the DGF due to its spectrally neutral profile.

## Custom Lux Equation

The spectral correction terms in the lux characterization equation are determined through piecewise linear regression, using predicted VIS and IR basic counts derived from Spectrilight SPD data.

Starting from the main model equation:

$$lux = \frac{DGF}{A_{time}} (C_0 VIS_{norm} + C_1 IR_{norm})$$

Because the predicted counts from Spectrilight are already normalized to basic counts (i.e., integration time included), the equation simplifies:

$$lux = DGF (C_0 VIS_{basic} + C_1 IR_{basic})$$

To perform linear regression, the equation is rearranged into point-slope form:

$$\frac{lux}{VIS_{basic} * DGF} = C_1 \left( \frac{IR_{basic}}{VIS_{basic}} \right) + C_0$$

- $y = \frac{lux}{VIS_{basic} * DGF}$
- $x = \frac{IR_{basic}}{VIS_{basic}}$
- $m = C_1$
- $b = C_0$

This form enables regression of lux against IR/VIS ratio, fitting coefficients across different spectral domains.

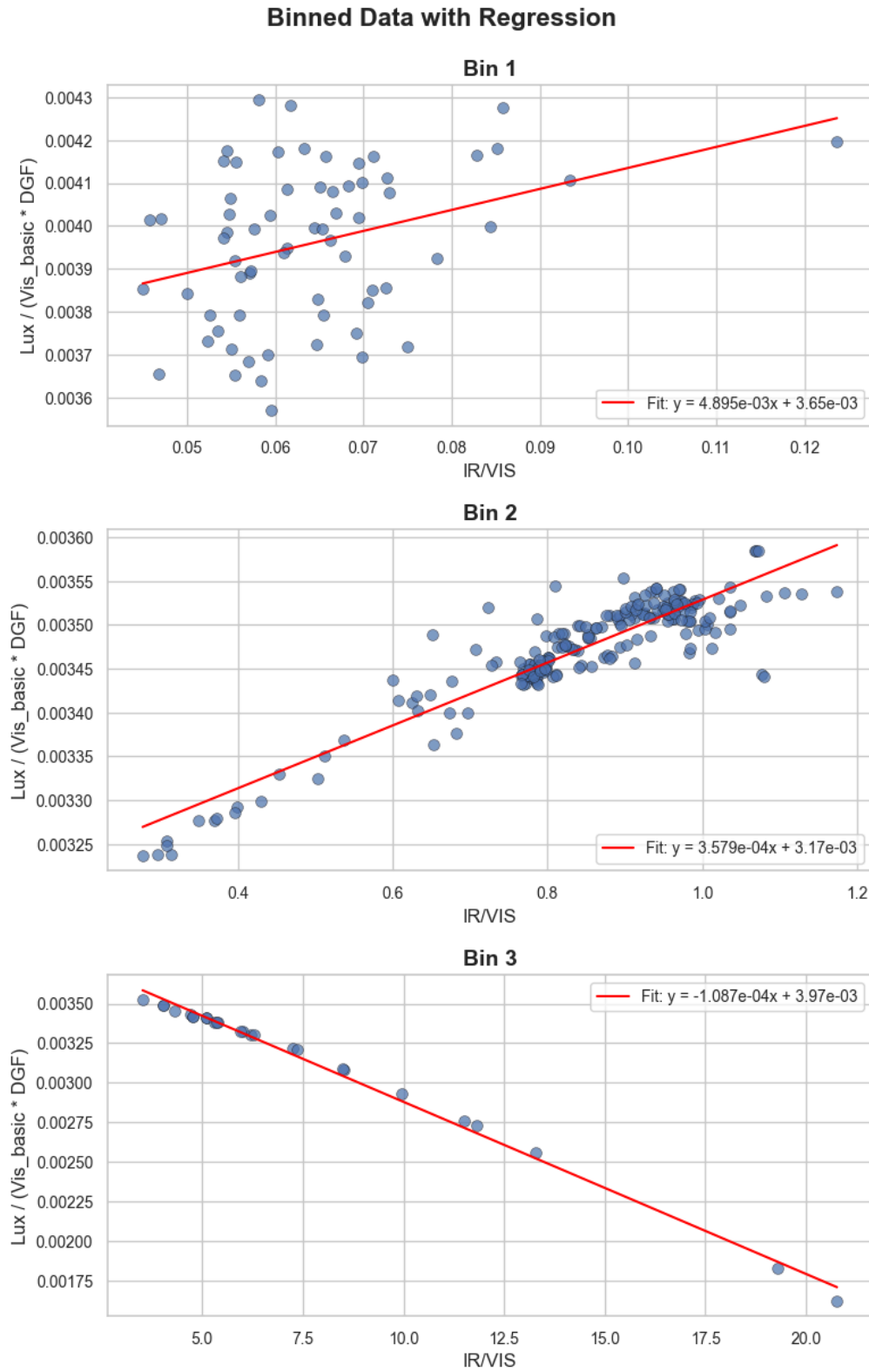
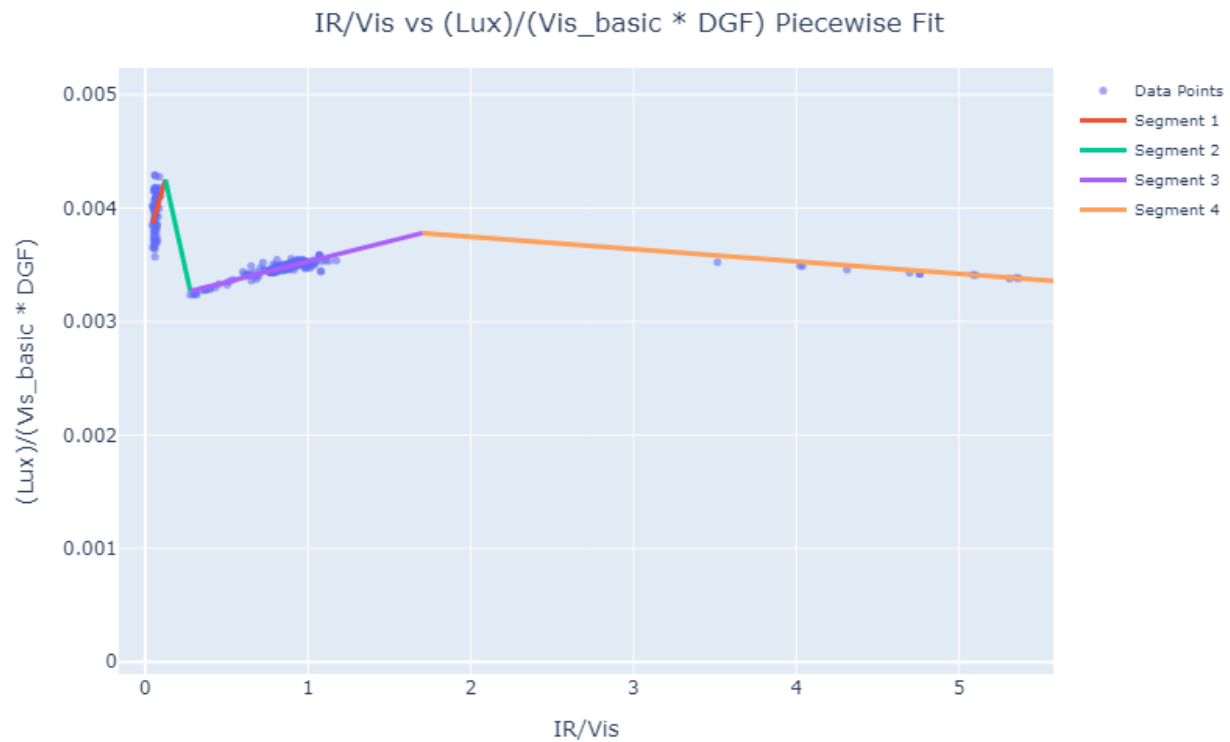


**Figure 10:** Linear regression line fits for the binned data.

To ensure continuity between domains, a transition segment is introduced between Sections 1 and 2, where the linear segments would otherwise not intersect. Four total line fits are used. The IR/VIS axis is truncated at 5 for clarity.



```
Segment 1: x ∈ [0.045, 0.124), C0 = 0.00365, C1 = 0.00490
Segment 2: x ∈ [0.124, 0.277), C0 = 0.00504, C1 = -0.00641
Segment 3: x ∈ [0.277, 1.705), C0 = 0.00317, C1 = 0.00036
Segment 4: x ∈ [1.705, 20.767), C0 = 0.00397, C1 = -0.00011
DGF: 16.666682 lux * ms / counts
```

**Figure 11:** Final piecewise lux equation and coefficients.

## Firmware Formulation

For use in embedded firmware, coefficients  $C_0$  and  $C_1$  are scaled by a factor of 128. This reflects a convention where normalized values in firmware are 128× smaller, due to gain ratio scaling applied to gain indices.

```

Calibration summary saved to calibration_segments.csv
Calibration Summary: (C0 AND C1 MULTIPLIED BY 128 FOR FW DEPLOYMENT):
-----
segment x_start  x_end  C0    C1    DGF
  1    0.045  0.124 0.467  0.627 16.667
  2    0.124  0.277 0.646 -0.820 16.667
  3    0.277  1.705 0.406  0.046 16.667
  4    1.705 20.767 0.508 -0.014 16.667

```

**Figure 12:** Lux piecewise equation coefficients scaled for FW convention.

The final lux equation implemented in firmware is the following:

$$\text{lux} = \begin{cases} 16.6667 \left( 0.4666(VIS_{norm, fw}) + 0.6266(IR_{norm, fw}) \right) / \text{atime} & 0 \leq \frac{IR_{norm, fw}}{VIS_{norm, fw}} < 0.1237 \\ 16.6667 \left( 0.6546(VIS_{norm, fw}) - 0.8202(IR_{norm, fw}) \right) / \text{atime} & 0.1237 \leq \frac{IR_{norm, fw}}{VIS_{norm, fw}} < 0.2769 \\ 16.6667 \left( 0.4058(VIS_{norm, fw}) + 0.0458(IR_{norm, fw}) \right) / \text{atime} & 0.2769 \leq \frac{IR_{norm, fw}}{VIS_{norm, fw}} < 1.7045 \\ 16.6667 \left( 0.5080(VIS_{norm, fw}) - 0.0139(IR_{norm, fw}) \right) / \text{atime} & \frac{IR_{norm, fw}}{VIS_{norm, fw}} \geq 1.7045 \end{cases}$$

## Model Error Analysis

This section evaluates the performance of the lux characterization equation using the same controlled dataset that was used to develop and fit the equation. The analysis reflects the model's accuracy under conditions it was explicitly trained to handle.

It is important to note that this is not an evaluation of real-world performance in uncontrolled or dynamic environments. In practice, higher errors may occur in scenes with mixed lighting (e.g. daylight combined with artificial sources or partially shaded regions). Such errors represent true model limitations resulting from unmodeled spectral combinations, compounded by the inherent limitations of using only two sensor channels to approximate the full spectral content of a scene.

Additionally, differences in field of view or placement between the sensor and a reference device may lead to discrepancies in reported lux. These are not model errors, but rather expected physical differences in the light each device receives.

### Agreement with Trusted Lux (Log-Log Domain)

To assess how well the model generalizes across light levels, the predicted lux values are compared to trusted lux values derived from Spectralight SPD integration. This comparison is plotted on a log-log scale to capture behavior across five orders of magnitude.

Figure 13 shows this comparison as a scatter plot, with a 1:1 reference line indicating ideal agreement. Since lux estimation is fundamentally an order-of-magnitude problem, the log scale provides a meaningful view of performance. When viewed this way, the model demonstrates excellent alignment across a wide dynamic range.

The tight clustering of points along the 1:1 line confirms that the model scales appropriately with intensity and maintains low relative error at both extremes of the range. Deviations from the line are primarily attributed to residual spectral mismatch, rather than issues with overall scaling or signal magnitude.

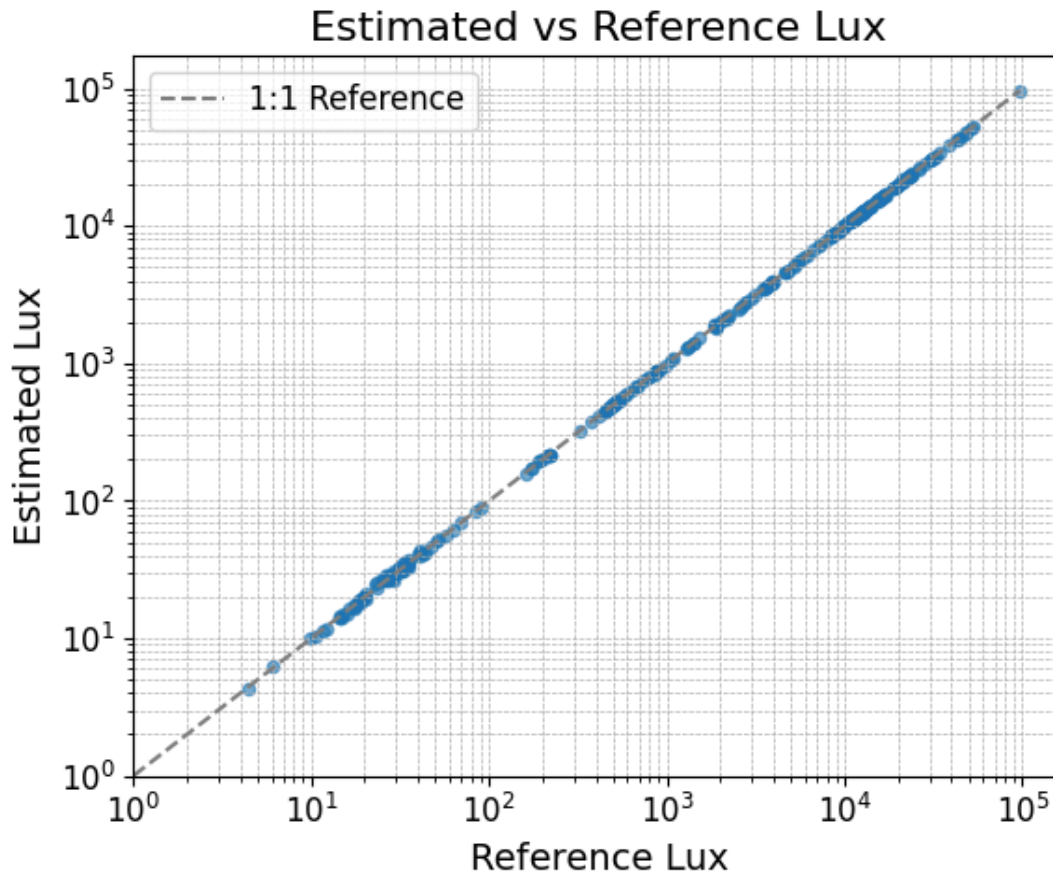


**Figure 13:** Log-log scatter plot of predicted lux vs. trusted lux under controlled single-source lighting.

## Spectral Dependency of Lux Predictions

While Section 10.1 highlights the model's accuracy across light intensity, this section focuses on spectral sensitivity, specifically how model behavior varies as a function of the IR/VIS ratio—a proxy for spectral shape and color temperature.

Figure 14 plots predicted lux against the IR/VIS ratio, using a linear x-axis. Each point is colored by the correlated color temperature (CCT) of the light source, illustrating how CCT generally decreases as IR/VIS increases within a given lighting type.

Notably, the largest deviations from expected lux occur under LED and fluorescent sources, which typically emit little to no infrared. While this reduces the influence of IR leakage through the VIS channel, it also limits the model's ability to apply meaningful spectral correction—since the IR channel carries little information—ultimately leading to higher prediction error in these cases.

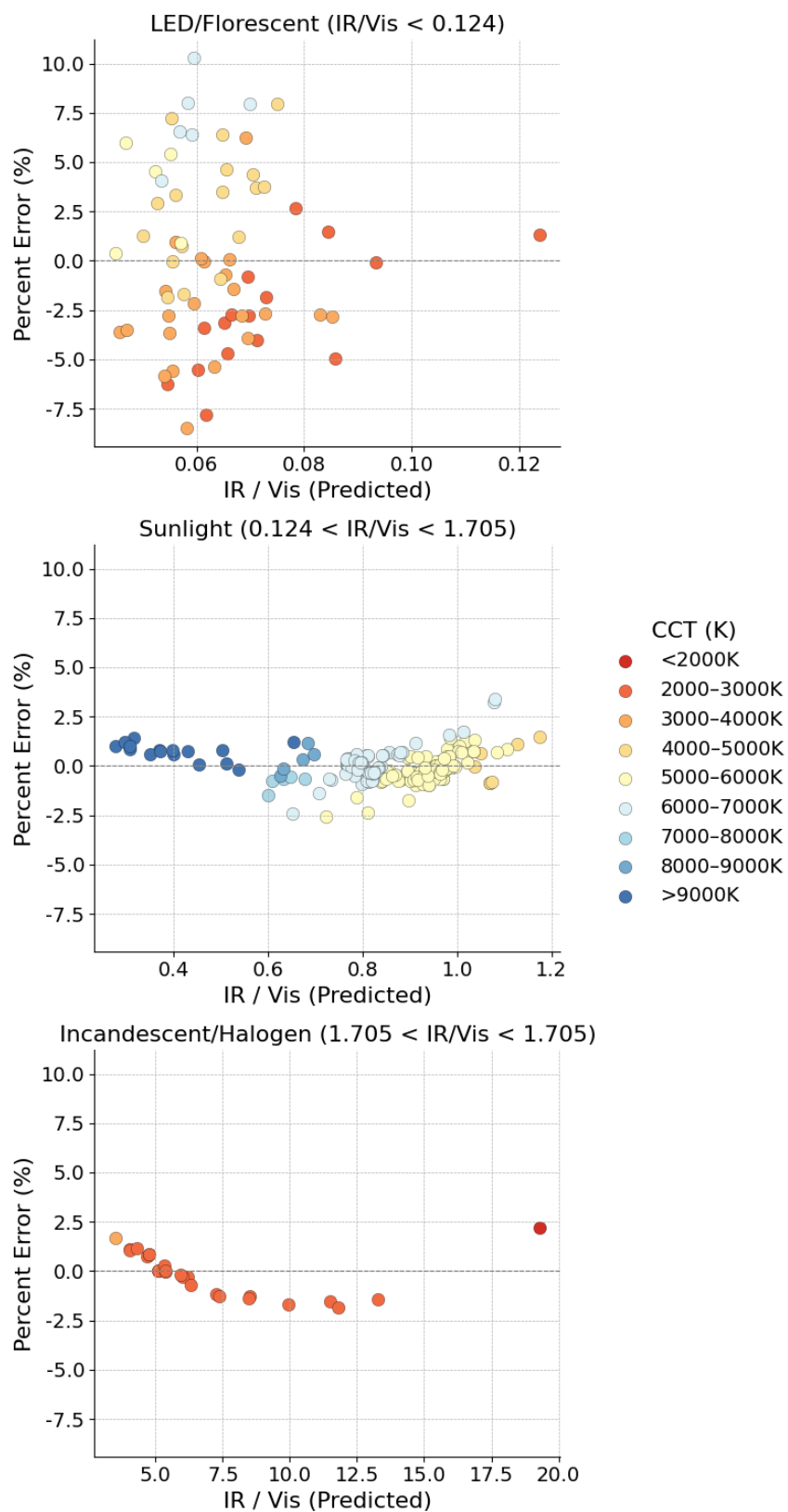


**Figure 14:** Predicted lux vs. IR/VIS ratio, plotted on a linear x-axis and colored by correlated color temperature (CCT).

## Challenges with Mixed or Atypical Lighting

In real-world environments, light from sources with different spectral shapes (e.g., daylight combined with LED) may overlap, producing conditions that fall outside the characterization dataset and potentially result in higher prediction error. Although mixed lighting data was not included during model development, the model's real-world performance was qualitatively evaluated by overlaying live lux readings onto a GoPro video feed during transitions between mixed lighting environments. In these observations, lux values remained physically reasonable and transitioned smoothly across scenes, suggesting that the model produces robust estimates even under complex, dynamic lighting conditions.

## Device-to-Device Variation (Not Included)

This analysis was performed using a single, golden unit device. Although all deployed units are calibrated to produce consistent VIS and IR counts (via per-unit gain factors), this does not account for any differences in the shape or shifting of the device's response curve between units.

These differences are not included in this document but should be considered if a high degree of lux accuracy across units is needed.

## Physical Measurement Differences

Finally, it is important to reiterate that not all differences between sensor output and reference device readings are model errors. Differences in the following can all lead to measurable differences in reported lux against a trusted device:

- Field of view (FOV)
- Orientation and placement
- Local light reflections or occlusions
- Uniformity of the light field

These are physical discrepancies in measurement context, not model shortcomings, and will be observed even if the characterization model is perfectly applied.

The VEET device has a narrower FOV than many standard lux meters. This means it captures a more constrained portion of the light field, which may lead to lower lux readings in diffuse or multi-source environments. These differences are not model errors but reflect true variation in light received at the sensor aperture. As such, interpretation of lux values should always consider the optical geometry of the device.

## Conclusion

This characterization model builds on the manufacturer's approach to improve lux estimation by addressing known sources of error, including spectral mismatch and optical attenuation. While performance is strongest under broadband sources with both VIS and IR content, light sources with limited IR—such as LEDs and fluorescents—tend to produce the largest errors due to the model's reduced ability to apply spectral correction.

When interpreting lux values from the VEET, it is important to consider the device's narrow field of view, which differs from that of traditional wide-angle lux meters. Significant discrepancies between VEET and trusted instruments can occur if FOV and light uniformity are not carefully controlled during comparisons.

The model was developed using ideal, single-source lighting and does not explicitly handle mixed spectral conditions, which may result in increased error under real-world use. It also assumes a consistent spectral response across all devices based on a single golden unit. While variations are expected to be small due to consistent optical packaging, minor unquantified device-to-device differences may still introduce additional error.

Lux estimation is fundamentally an order-of-magnitude problem, and when viewed in this context, the model demonstrates excellent alignment across a wide range of light sources.

Despite its limitations, qualitative validation—including real-time observation under dynamic, mixed lighting—showed smooth transitions and physically meaningful lux values, indicating the model performs reliably within the constraints of the sensor hardware.

For applications requiring higher absolute accuracy or broader spectral coverage, lux should be derived from a sensor with more spectral channels or a full SPD measurement.